

POLYCAPILLARY OPTICS BASED NEUTRON FOCUSING FOR SMALL SAMPLE NEUTRON CRYSTALLOGRAPHY

W.M. Gibson^a, H.H. Chen-Mayer^b, D.F.R. Mildner^b, H.J. Prask^b, A.J. Schultz^c, R. Youngman^a, T. Gnäupel-Herold^b, M.E. Miller^c, and R. Vitt^c

a) X-Ray Optical Systems, Inc., Albany, NY, b) National Institute of Standards and Technology, Gaithersburg, MD, c) Argonne National Laboratory, Argonne, IL

ABSTRACT

This work presents preliminary measurements designed to explore a new approach to neutron diffraction that is somewhat analogous to the pseudo-Laue technique, except that instead of using a broad energy (wavelength) bandwidth it uses a broad angular bandwidth. We have used a polycapillary focusing optic to focus neutrons from a monochromatic beam (using the BT-8 spectrometer on the NIST research reactor) and from a polychromatic beam at a pulsed spallation source (the Intense Pulsed Neutron Source, IPNS at Argonne National Laboratory) into a small, intense spot and have carried out preliminary diffraction measurements. Using the single crystal diffraction (SCD) facility on IPNS, diffraction of a 3° convergent beam from an alpha quartz crystal showed six diffraction beams in the 1-5 Å wavelength bandwidth transmitted by the optic. The diffraction spots showed an intensity gain of 5.8 ± 0.9 compared to a direct beam diffracting from the same sample volume as that illuminated by the convergent beam.

1. INTRODUCTION

Rapid, accurate, high-resolution structural analysis of proteins is central to the success of rational drug design and other medical and scientific applications. Neutron diffraction has powerful and unique potential for determination of the structure and dynamics of proteins including direct determination of hydrogen positions, solvent association, etc. (Timmins, 1995). However, the low intensity, broad energy (wavelength) bandwidth and large angular spread of neutron beams and the limited availability of neutron sources have kept this potential from being realized. A particularly serious limitation arises from the small size of the crystals available for medically important proteins.

Other cases that involve the use of small crystals or small sampling areas include strain or phase distributions in metals (for example, at welds), and measurement of the structure and phase changes of materials at high pressure or low temperature. Also, mapping of composition in lateral directions by prompt neutron activation analysis requires small size, high intensity neutron beams.

Another important feature of neutron diffraction arises from the lower energy of neutrons compared to that of X-rays of the same wavelength. For example a 0.034 eV neutron and an 8.03 keV X-ray both have a wavelength of 1.54 Å. This leads to reduced radiation damage during neutron irradiation and therefore longer crystal lifetime during diffraction measurements which, among other things, reduces the need to cool the crystal during the measurement. Also the penetration (or scattering mean-free-path) of neutrons is much greater than for x rays and the lower attenuation reduces anisotropic absorption effects for plate-like or rod-like crystals that often leads to errors in x-ray analysis which are sometimes difficult to eliminate. In addition, because neutrons scatter from the nuclei, the scattering power for neutrons does not fall off dramatically with scattering angle as does X-rays. This means that higher resolution data should be easier to obtain with neutron diffraction.

The "pseudo-Laue" method has been used to permit a wide wavelength bandwidth to be used with either a reactor-based source (Wilkinson, 1991) or a pulsed spallation source (Schoenborn, 1992a). In addition to providing a larger usable neutron intensity, this technique samples a larger volume of reciprocal space on each exposure, therefore, requiring fewer exposures to cover the angular space necessary for a structure determination.

The work reported here represents preliminary measurements designed to explore a new approach that is somewhat analogous to the pseudo-Laue technique except that instead of using a broad energy (wavelength) bandwidth it uses a broad angular bandwidth. We have used a polycapillary focusing optic to focus neutrons from a monochromatic beam (using the BT-8 spectrometer on the NIST research reactor) and from a polychromatic beam at a pulsed spallation source (the Intense Pulsed Neutron Source, IPNS at Argonne National Laboratory) onto a small, intense spot and have carried out preliminary diffraction measurements on IPNS.

Polycapillary optic focusing of cold neutrons has been shown to be effective, giving intensity gains of nearly 100 x and spot sizes $\sim 500 \mu\text{m}$ (Chen, 1992; Xiao, 1994). Convergent beam x-ray crystallography has already been demonstrated for protein crystals with lattice constants up to 70 \AA with a resolution better than 2 \AA (Owens, 1996; Huang, 2001). It is the combination of these developments that form the basis for enhanced neutron-based small-sample crystallography, the initial stages for which are described in this paper. The use of a convergent beam results in elongated diffraction spots that require modified software for analysis (Ho, 1998). Contrary to simple expectation, this elongation does not result in an untenable overlap problem, even for protein crystals. Aside from low index orientations, the diffraction "streaks" are displaced from each other, and provided that the streak widths are small compared to their separation they can be independently integrated and indexed (Ho, 1998). The widths of the diffraction streaks are determined by the mosaic spread of the crystal and the sample (or beam) size. The pseudo-Laue technique also produces elongated diffraction spots (Schoenborn, 1992b), although these differ in nature from those produced by a convergent beam.

Enhanced neutron intensity at the focal spot can be used to increase the integrated intensity in the diffraction spots and also increase the reciprocal space sampled in each exposure. Both of these effects increase the efficiency for neutron diffraction structure determinations. Of particular importance is the fact that the smaller sample size ($<500 \mu\text{m}$) can greatly increase the number and types of proteins or other molecules that can be studied. The reduced sample size also reduces the width of the diffracted spots, allowing the sample-to-detector distance to be reduced, so that all of the diffracted spots needed for each crystal position can be measured simultaneously. These effects, taken together, have the potential to dramatically increase the opportunity and accessibility for neutron diffraction analysis especially for biological macromolecules. It should be noted that the efficiency for polycapillary focusing of neutrons depends on the neutron wavelength. At present, effective focusing can be done only for neutrons with $\lambda > \sim 1 \text{ \AA}$, and is therefore less useful for measurement of small molecules than for medium to large molecules. Such cases, however, are where the need is greatest because of the difficulty of growing large, highly perfect crystals of macromolecules and because of their lower scattering strength.

In summary, the potential benefits of polycapillary-based convergent beam neutron crystallography include smaller crystal size, larger sampled reciprocal space, higher neutron current density on small samples, and smaller diffracted spot widths, allowing the detector to be closer to the sample and therefore measure a larger solid angle subtended at the sample. This paper reviews a preliminary study of these potential benefits.

2. EXPERIMENTAL RESULTS

A. Monolithic polycapillary optic

The principles and schematic structure underlying the operation of a monolithic polycapillary focusing optic are shown in Fig. 1. The optic fabricated for this project has the following characteristics: length, 75 mm; cross section, hexagonal; input, 7.4 mm flat-to-flat; output, 5.6 mm; channel size at input, $8.8 \mu\text{m}$; output focal distance, 98 mm; transmission efficiency for $\text{CuK}\alpha$ x-rays (8.1 keV), 24.7 % (x rays out/x rays in)(measured in reverse, collimating, geometry). A photograph of the enclosed optic is shown in Fig. 2.

The optic was mounted in a high precision, remotely controlled alignment system with five degrees of freedom: three orthogonal translations, with 25 mm range and 10 μm precision; and two orthogonal angular motions, θ_x , and θ_y , with 0.25 mrad (0.0014 $^\circ$) precision.

B. Focusing of monochromatic neutrons.

Measurements were performed on the BT-8 beam line at the 20 MW NIST Research Reactor at five different neutron wavelengths; 1.08 \AA , 1.40 \AA , and 1.67 \AA , using diffraction from a (220) copper monochromator crystal; and 2.40 \AA and 3.10 \AA from a (200) copper monochromator crystal. The gain of the optic at each neutron wavelength was obtained from the ratio of the number of neutrons within the full-width-at-half-maximum (FWHM) for a Gaussian distribution fitted to the measured peak to the number of neutrons within the same size spot without the optic. A summary of all of the

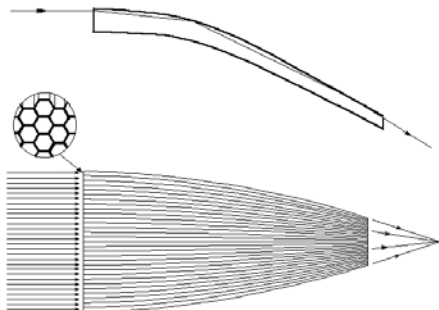


Figure 1. Schematic of polycapillary monolithic focusing optic.

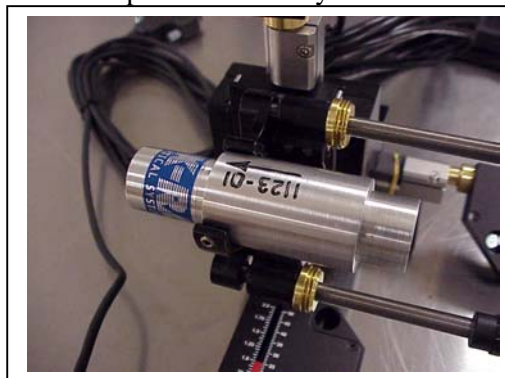


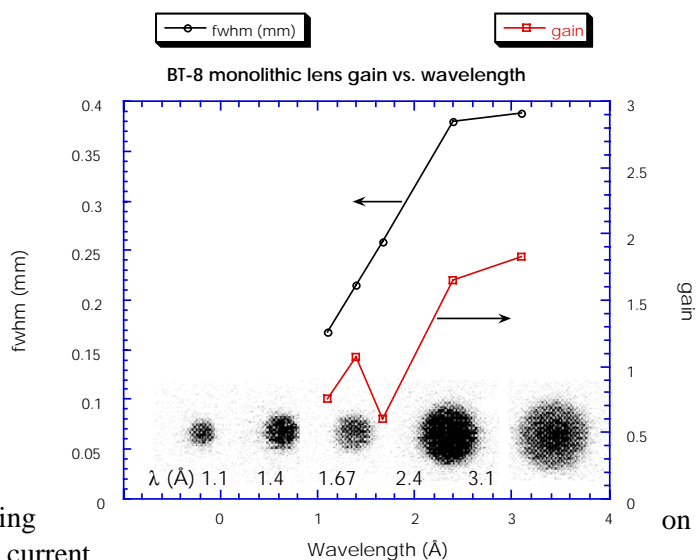
Figure 2. Photograph of neutron focusing optic mounted in the alignment jig.

measurements of the optic gain and the focal spot size for each neutron wavelength is shown on Fig. 3. The gain measurement for 1.67 \AA neutrons is low because of imprecise alignment for that measurement and the FWHM for 3.1 \AA neutrons is affected (reduced) by the presence of higher order 1.55 \AA neutrons. The transmission efficiency and therefore the gain of the optic is strongly dependent on the angular distribution of the neutron beam at the optic input.

Figure 3. Summary of measurements with the neutron focusing optic 1123-01 on the NIST BT-8 Spectrometer with a Cu diffraction crystal.

C. Focusing of polychromatic neutrons.

Measurements were made with the same optic on the single crystal diffractometer (SCD) beam line at (IPNS) at Argonne National Laboratory. The source operates at 30 Hz with 450 MeV protons in 0.3 μs wide pulses impinging a depleted uranium target with a time-averaged current of 15 μA . The SCD beam line views a 100 mm wide liquid methane moderator at a distance of 9.5 meters. This means that the neutron angular divergence at the input to the SCD instrument is less than ± 5 mrad, which is a better match to the acceptance angle for the neutron focusing optic than the beam from



the NIST BT-8 spectrometer, especially for the longer wavelength portion of the $0.5 \text{ \AA} - 5.0 \text{ \AA}$ wavelength bandwidth. The transmission through the optic was determined by computer simulation calculations using the measured neutron spectrum and angular distributions. The transmission efficiency of the optic as a function of the incident neutron wavelength was also calculated. For both the calculations and the measurements a 6 mm aperture defined the beam size at the entrance to the optic. Figure 4 shows the results of this calculation, which assumes that the same input angular distribution applies for all wavelengths. These results can be approximated over the wavelength range $1.5 \text{ \AA} < \lambda < 6 \text{ \AA}$ by the expression $[8.3 \lambda - 9.8]/90$.

Applying the results of Fig. 4 and the measured input neutron spectrum, it is possible to obtain the neutron wavelength spectrum for neutrons exiting the optic (in the focal spot). This is shown in Fig. 5. In addition to the focal spot, there was a background of high-energy (short wavelength) neutrons. The measured focused neutron-to-background ratio (within the FWHM) of the focal spot was 20.0 ± 1.5 . From scans of the focal spot, the measured spot width **FWHM** = $413 \pm 13 \text{ \mu m}$, and after a small correction for the high-energy neutron background the **Gain** = 3.96 ± 0.32 . Measurements were also made with a 127 mm Be absorber in the beam just before the optic. This removes neutrons with wavelength $\lambda < 4 \text{ \AA}$. For this condition the measured **FWHM** = $836 \pm 39 \text{ \mu m}$ and the **Gain** = 5.43 ± 0.23 .

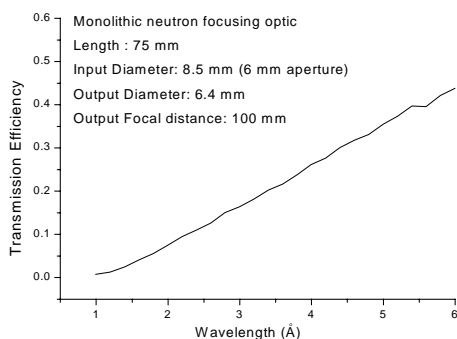


Figure 4. Simulated transmission vs neutron wavelength.

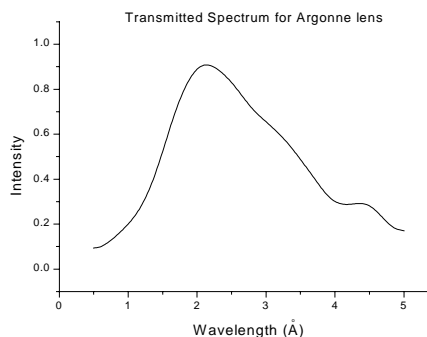


Figure 5. Spectrum of focused neutrons from optic on IPNS-SCD

D. Diffraction measurements.

Preliminary single-crystal time-of-flight neutron diffraction data were measured using the IPNS single crystal diffractometer (SCD) (Schultz, 1984; Schultz, 1993) equipped with a position-sensitive ^6Li -glass scintillation area (300 mm x 300 mm) detector. Because of the pulsed nature of the source, neutron wavelengths are determined by time-of-flight based on the de Broglie equation $\lambda = (h/m) \cdot (t/l)$, where h is Planck's constant, m is the neutron mass, and t is the time-of-flight for a total flight path l , so that the entire thermal spectrum of neutrons can be used. With a position-sensitive area detector and a range of neutron wavelengths, a solid volume of reciprocal space is sampled with a stationary orientation of the sample and the detector. A schematic representation of the IPNS SCD is shown in Figure 6.

A single crystal of alpha-quartz was aligned in the neutron beam at the normal crystal position. The crystal had approximate dimensions of $3 \times 2 \times 2 \text{ mm}^3$; thus, it was about 30 times larger than the focused beam. Time-of-flight Laue diffraction data were collected in a wavelength range of $0.7 \text{ \AA} - 4.2 \text{ \AA}$. With the optic, six diffraction peaks were observed after 16.7 hours, all with wavelengths between 1.5 \AA and 3.1 \AA . A selected time slice through the diffraction peak at $\lambda = 2.4 \text{ \AA}$ is contoured in Figure 7a. For comparison, Figure 7b shows the same peak obtained after 1.5 hours without the optic. The ratio of sample volumes illuminated by the incident neutron beam with and without the optic of 1:30 between 7a and 7b accounts for the different measurement times.

Peak profiles for the same two peaks are shown in Figure 8. These closely approximate a typical 2θ scan from a conventional diffractometer. In this case, each count for a particular X channel was summed over the Y and TOF channels. The higher background in Figure 8a relative to 8b is primarily due to the longer counting time of 16.7 hours versus 1.5 hours. Each peak was fit to a Gaussian shape from which the derived FWHM values are 2.2 channels without the optic (8b) and 4.5 channels with the optic (8a).

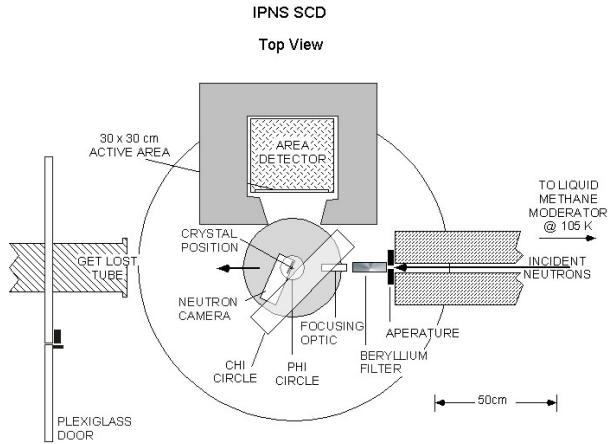


Figure 6. Schematic representation of the IPNS Single Crystal Diffractometer (SCD). The moderator-to-sample distance is 9340 mm and the sample-to-detector distance is 320 mm.

Figure 7. Contours of quartz Bragg peaks. Each channel (pixel) spans about 9.4 millirad. Contour increments are 30 counts starting at 15. a) Peak from quartz crystal with optic. b) Peak without optic.

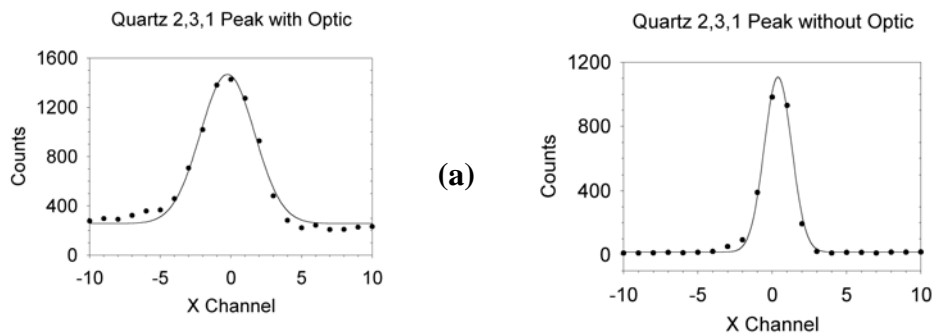
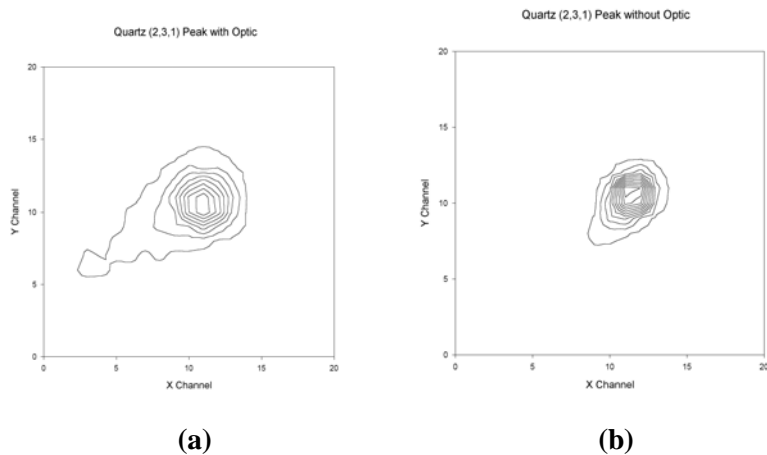


Figure 8. Plots of the detector horizontal scan for peaks a) with and b) without the focusing optic. Each point is integrated over the vertical channels and the time channels. for this peak. The solid line is a Gaussian fit to each peak.

Integration of the peak intensities for 8a and 8b, normalized to the same sampling volume and sampling time shows a gain of 5.8 ± 0.9 for the focusing optic compared to a measurement on a small ($500 \mu\text{m}$

diameter) sample without the optic. This is larger than the gain of 4.0 ± 0.3 measured with the entire incident beam. The difference may be due to the single wavelength region at 2.4 \AA which could give a higher transmission efficiency and a larger sampling volume than used for the gain calculation (included in the estimated uncertainty of this value).

3. CONCLUSIONS

The diffraction measurement carried out in this study was designed only to explore the feasibility of using a convergent beam for diffraction. It is clear that for a sample size much greater than 0.5 mm and small lattice constant crystal such as the quartz crystal used, the optic offers no particular benefit. The wavelength range sampled (1.5 \AA – 4 \AA as shown in Fig. 5) included only 6 diffraction peaks (compared to 39 when the entire spectrum is used). However these results show that although the convergent beam broadens the diffraction peaks as expected, this is not serious. The intensity gain observed in the focused beam incident on the sample is also present in the diffracted beams. This demonstrates the feasibility of applying a convergent beam to small sample diffraction measurements.

The total convergence angle of the beam used in these studies was $\sim 3^\circ$. The neutron current density and therefore the optic gain can be further increased by decreasing the output focal distance of the optic. Recently, a monolithic neutron focusing optic was made with an output focal distance of 20 mm . This optic has been studied using the cold neutron beam at the NIST reactor and gave a focal spot size of $100 \text{ }\mu\text{m}$ and gain of 46 (with an effective convergence angle of $\sim 6^\circ$). We plan to investigate the use of this optic and perhaps even stronger focusing optics for neutron diffraction.

4. ACKNOWLEDGEMENTS

The identification of commercial materials and instruments in this paper is for an adequate description of the experimental facilities and procedures; it does not imply recommendation or endorsement by the National Institute of Standards and Technology, nor does it imply that the materials and equipment are necessarily the best available for the purpose.

Work at Argonne National Laboratory was supported by the US Department of Energy, Office of Basic Energy Sciences, Division of Materials Sciences, under contract No. W-31-109-ENG-38. This work was also supported in part by the US Department of Energy through Argonne National Laboratory under contract OF-01385, and has benefited from the results of work supported by NASA under contract #NCC8-125. We also thank the NIST Center for Neutron Research for the use of the BT-8 instrument.

4. REFERENCES

- Chen, 1992;** H.H. Chen, R.G. Downing, D.F.R. Mildner, W.M. Gibson, M.A. Kumakhov, I.Yu. Ponomarev, and M.V. Gubarev, "Guiding and Focusing Neutron Beams using Capillary Optics", *Nature*, **357**, 391-3 (1992)
- Ho, 1998;** J.X. Ho, E.H. Snell, R.C. Sisk, J.R. Ruble, D.C. Carter, S.M. Owens, and W.M. Gibson, "Stationary Crystal Diffraction with a Monochromatic Convergent X-ray Source and Application for Macromolecular Crystal Data Collection", *Acta. Cryst.*, **D54**, 200-214 (1998)
- Huang, 2001;** H. Huang, C.A. MacDonald, W.M. Gibson, I. Ponomarev, D.C. Carter, J.X. Ho, J.R. Ruble, J. Chik, and A. Parsegian, "Focusing Polycapillary Optics for Diffraction" Proc. 50th Annual Denver X-Ray Conference (these proceedings) (2001)
- Owens, 1996;** S.M. Owens, J.B. Ullrich, I.Yu. Ponomarev, D.C. Carter, R.C. Sisk, J.X. Ho, and W.M. Gibson, "Protein Crystal Structure Measurements Using Polycapillary X-Ray Optics", *SPIE Proc.*, vol. **2859**, 200-209 (1996)
- Schoenborn, 1992a;** B. P. Schoenborn, "Area Detectors for Neutron Protein Crystallography", *Proc. SPIE*, vol. **1737**, 235-243 (1992)

Schoenborn, 1992b; B. P. Schoenborn, Multilayer Monochromators and Supermirrors for Neutron Protein Crystallography Using a Quasi Laue Technique", *Proc. SPIE*, vol. **1738**, 192-198 (1992)

Schultz, 1984; A.J. Schultz, K. Srinivasan, R.G. Teller, J.M. Williams, and C.M. Lukehart, "Single Crystal Time-of-Flight Neutron Diffraction Structure of Hydrogen *cis*-Diacetyltetracarbonylrhenate, [*cis*-(OC)₄Re(CH₃CO)₂]H: A Metallaacetylacetonone Molecule", *J. Am. Chem. Soc.*, **106**, 999-1003 (1984)

Schultz, 1993; A.J. Schultz, *Trans. Am. Crystallogr. Assoc.*, **29**, 29-41 (1993)

Timmins, 1995; P.A. Timmins, "Structural Molecular Biology: Recent Results from Neutron Diffraction", *Physica B*, **213**, 26-30 (1995)

Wilkinson, 1991; C. Wilkinson and M.S. Lehmann, "Quasi-Laue Neutron Diffractometer", *Nucl. Instr. Meth.*, **A31**, 411-415 (1991)

Xiao, 1994; Q.-F. Xiao, H.H. Chen, V.A. Sharov, D.F.R. Mildner, R.G. Downing, N. Gao, and D.M. Gibson, "Neutron Focusing Optic for Submillimeter Materials Analysis", *Rev. Sci. Instrum.*, **65**, 3399-3402 (1994)